Supplementary Information

Large Energy Capacitive High-Entropy Lead-Free Ferroelectrics

Liang Chen[1], Huifen Yu[1,2], Jie Wu[1,2], Shiqing Deng[1,2], Hui Liu[1,2], Lifeng Zhu[3], He Qi[1,*] and Jun Chen[1,*]

[1] Beijing Advanced Innovation Center for Materials Genome Engineering, Department of Physical Chemistry, University of Science and Technology Beijing, Beijing 100083, China

[2] School of Mathematics and Physics, University of Science and Technology Beijing, Beijing 100083, China

[3] School of Materials Science and Engineering, University of Science and Technology Beijing, Beijing 100083, China

*Corresponding author. E-mail: qiheustb@ustb.edu.cn; junchen@ustb.edu.cn

Finite element simulation

The electric field and electric potential distribution as well as electric tree evolution were simulated by finite element methods with 2D models using COMSOL software. The simulated model is based on the SEM diagrams and the selected size is 16×24 μm^2. To simulate the dielectric breakdown behavior of the studied samples from low-entropy to high-entropy, a scalar field $s(x, t)$ was applied to represent the breakdown state, where s =1 means the initial state and s =0 means complete breakdown state (0≤ s ≤1). Since dielectric constant (ε_r) is a continuous function of s, the difference in ε_r is adopted to describe the breakdown state, which can be expressed as [1, 2]:

$$\varepsilon(s) = \frac{\varepsilon_{ini}}{f(s) + \psi} \tag{1}$$

where ε_{int} represents the initial ε_r, $f(s) = 4s^3 - 3s^4$, and ψ is 0.0001. In addition, the ferroelectric ceramics include grains and grain boundaries. The ε_r of grains is electric field-dependent following Johnson's approximation [3], and the ε_r of grain boundary is linear. Therefore, the ε_r of grains (ε_g) and grain boundaries (ε_{gb}) under a specific electric field is described by the following equation:

$$\varepsilon_{ini}(E) = \frac{\varepsilon_g(0)}{(1 + kE^2)^{1/3}} \tag{2}$$

$$\varepsilon_{ini}(E) = \varepsilon_{gb} \tag{3}$$

where k is 0.0013, and $\varepsilon_g(0)$ is the zero-field dielectric constant and is taken to be 750, 700, and 500 for low-entropy BNTFN-0, medium-entropy BNTFN-0.1, and high-entropy BNTFN-1/3 samples, respectively. Generally, the ratio of ε_g to ε_{gb} is set as 10:1 in this work [4, 5]. The theoretical model can be constructed by the following formulas:

$$\overline{\nabla}\left[\frac{1}{f(s) + \psi}\overline{\nabla\phi}\right] = 0 \tag{4}$$

$$\frac{\partial s}{\partial t} = -\frac{f'(s)}{2[f(s) + \psi]^2}\overline{\nabla\phi} \times \overline{\nabla\phi} + f'(s) + \frac{1}{2}\overline{\nabla}^2 s \tag{5}$$

Under the correct boundary and initial conditions, Eqs. (4) and (5) can be applied to the solution of dimensionless unknown fields $\phi(x, t)$ and $s(x, t)$. The simulated results are recorded in Fig. 5 and Fig. S8.

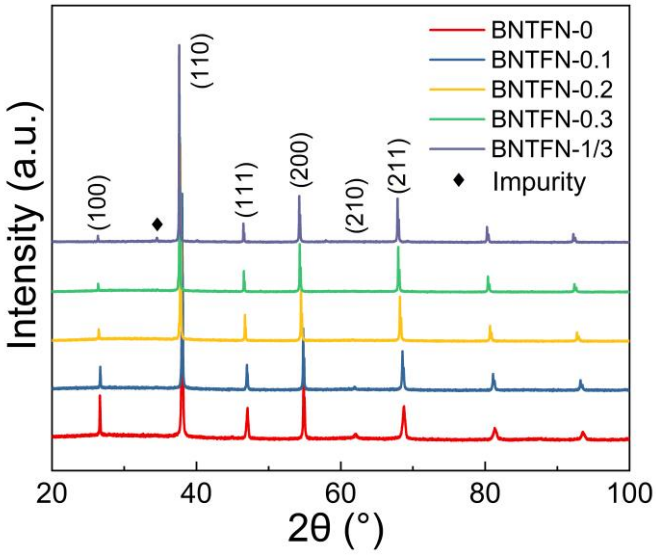

Fig. S1 The XRD patterns for BNTFN-*x* (*x*=0, 0.1, 0.2, 0.3, 1/3) ceramics

The XRD patterns of the studied samples indicate that BNTFN-0, BNTFN-0.1, BNTFN-0.2, and BNTFN-0.3 are pure perovskite structure. A small amount of impurity can be found in BNTFN-1/3 ceramics with pseudo-cubic phase.

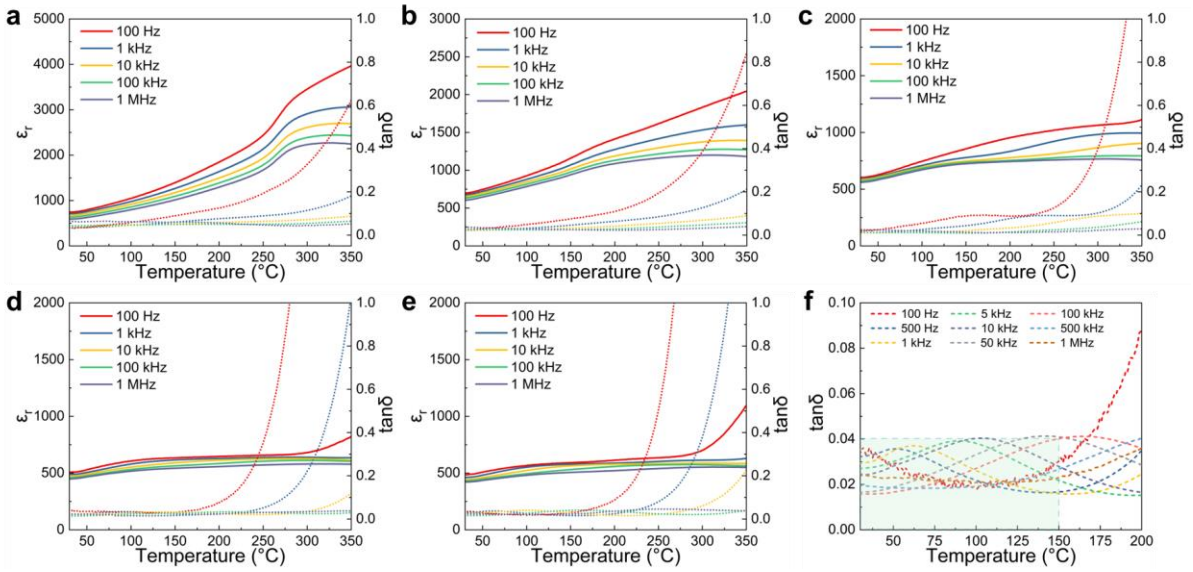

Fig. S2 Temperature-dependent ε_r and tanδ for **a** BNTFN-0 ceramics, **b** BNTFN-0.1 ceramics, **c** BNTFN-0.2 ceramics, **d** BNTFN-0.3 ceramics, and **e** BNTFN-1/3 ceramics. **f** Temperature-dependent tanδ for BNTFN-1/3 ceramics from 100 Hz to 1 MHz

As shown in Fig. S2a, BNTFN-0 ceramic shows normal ferroelectric features. With the introduction of Fe^{3+} and Nb^{5+}, enhanced diffuse phase transition behavior with flatten temperature-dependent ε_r spectra and decreased room-temperature ε_r are clearly found, implying the improved dielectric relaxation characteristic. Moreover, the decreased room-temperature ε_r also explains the delayed polarization saturation behavior.

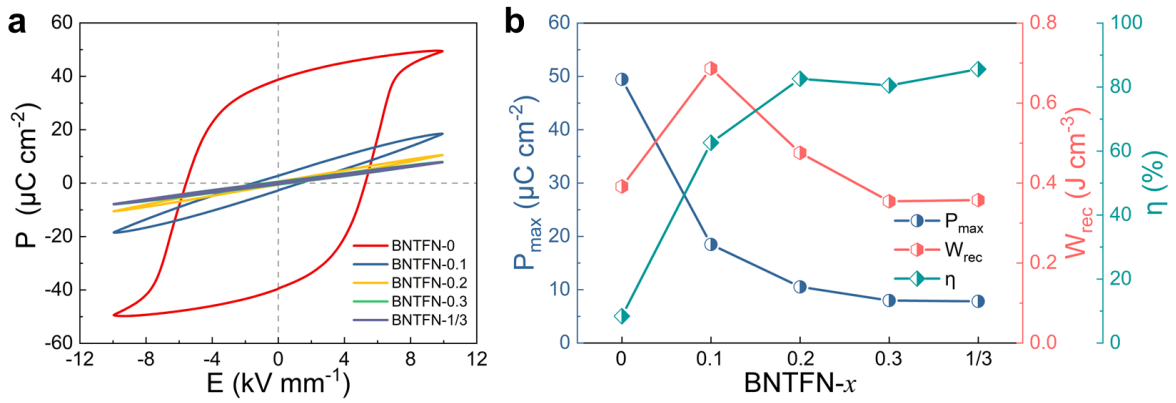

Fig. S3 a The bipolar *P-E* loops of BNTFN-*x* (*x*=0, 0.1, 0.2, 0.3, 1/3) ceramics under 10 kV mm^{-1}. **b** P_{max}, W_{rec} and η under 10 kV mm^{-1} for BNTFN-*x* (*x*=0, 0.1, 0.2, 0.3, 1/3) ceramics

With the introduction of Fe^{3+} and Nb^{5+}, the ferroelectric hysteresis loops gradually become slimer, presenting that the introduction of Fe^{3+} and Nb^{5+} can effectively break the long-range ferroelectric order and decrease energy loss. Furthermore, P_{max} under 10 kV mm^{-1} presents a similar downward trend to room-temperature ε_r, which is one of the important contributions of polarization. Notably, the ultralow P_{max} and W_{rec} in BNTFN-*x* (*x* =0.1, 0.2, 0.3, 1/3) ceramics are mainly caused by the insufficient external electric fields, which can be largely improved by high enough electric fields.

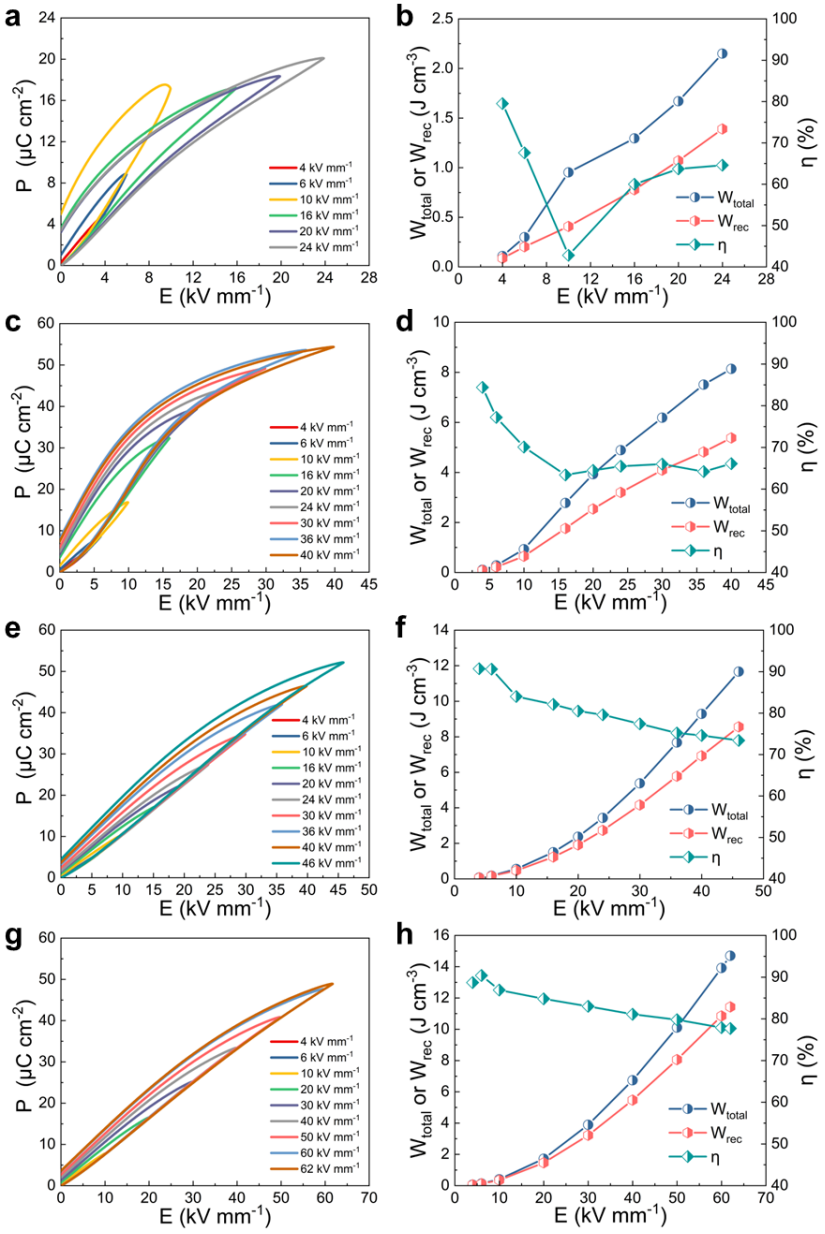

Fig. S4 The *P-E* loops, and W_{total}, W_{rec} and η from low electric field to E_b for **a-b** BNTFN-0 ceramics, **c-d** BNTFN-0.1 ceramics, **e-f** BNTFN-0.2 ceramics, and **g-h** BNTFN-0.3 ceramics

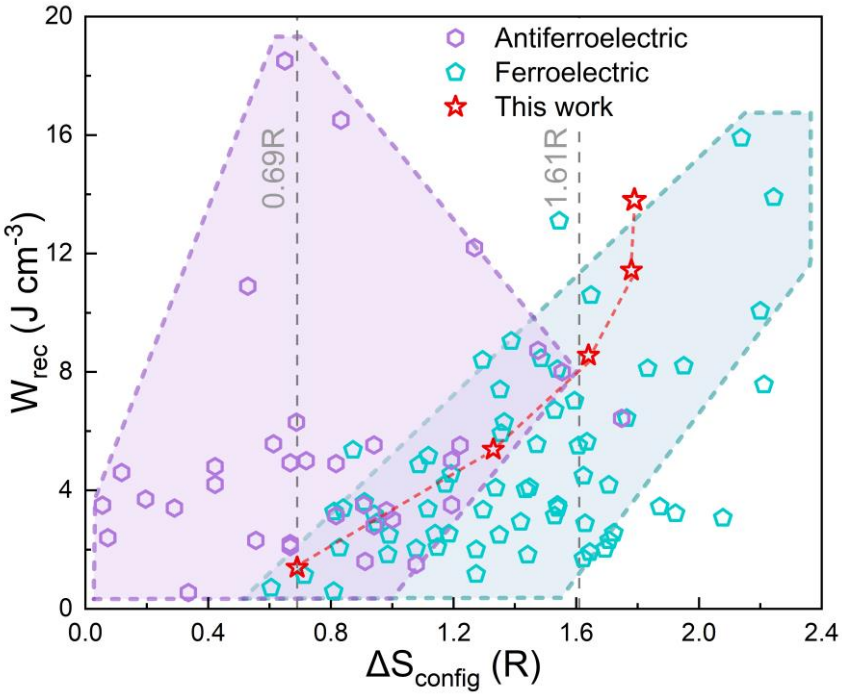

Fig. S5 A comparison of W_{rec} and ΔS_{config} between the studied samples in this work and other reported lead-free relaxor ferroelectric and antiferroelectric ceramics

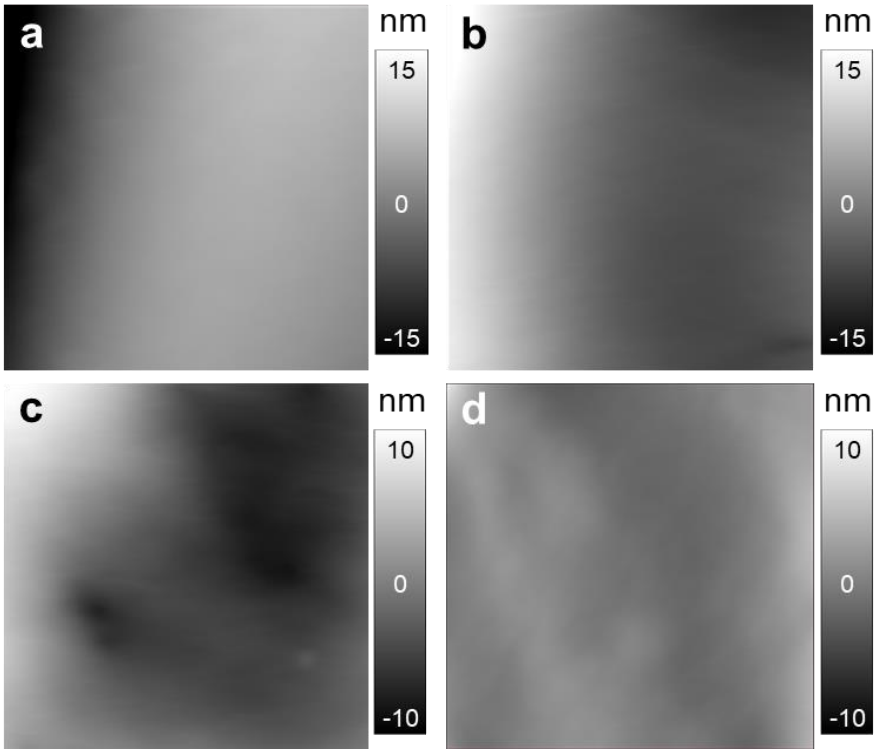

Fig. S6 Out-of-plane PFM morphologies within one grain for **a** BNTFN-0, **b** BNTFN-0.1, **c** BNTFN-0.2, and **d** BNTFN-1/3 ceramics

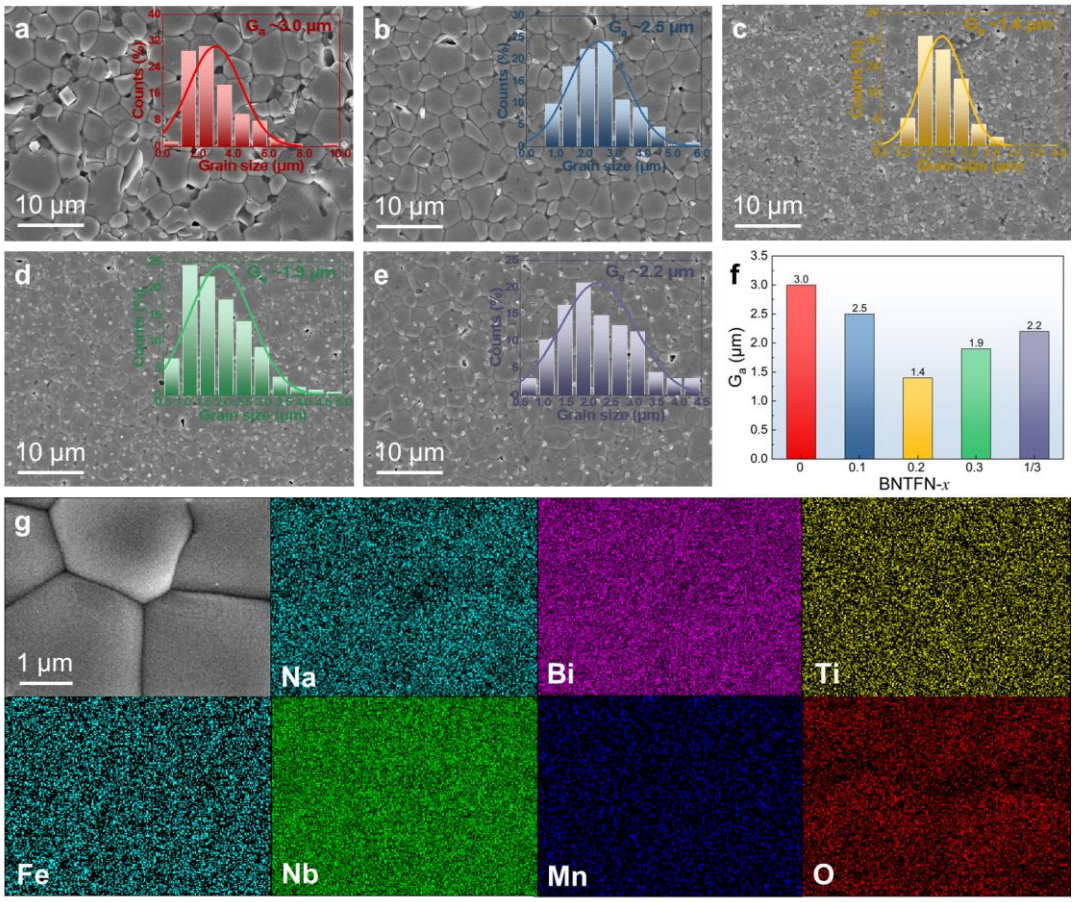

Fig. S7 Thermal etched SEM morphology and grain size distribution for **a** BNTFN-0, **b** BNTFN-0.1, **c** BNTFN-0.2, **d** BNTFN-0.3, and **e** BNTFN-1/3 ceramics. **f** G_a for BNTFN-x (x=0, 0.1, 0.2, 0.3, 1/3) ceramics. **g** Element distribution maps of BNTFN-1/3 ceramic

The element distribution maps of BNTFN-1/3 ceramic are performed in adjacent grains with triangular grain boundaries. Not only a densely contact grain boundary structure but also a uniform element distribution between the grains and grain boundaries can be clearly observed in the studied sample, proving a good sample quality again.

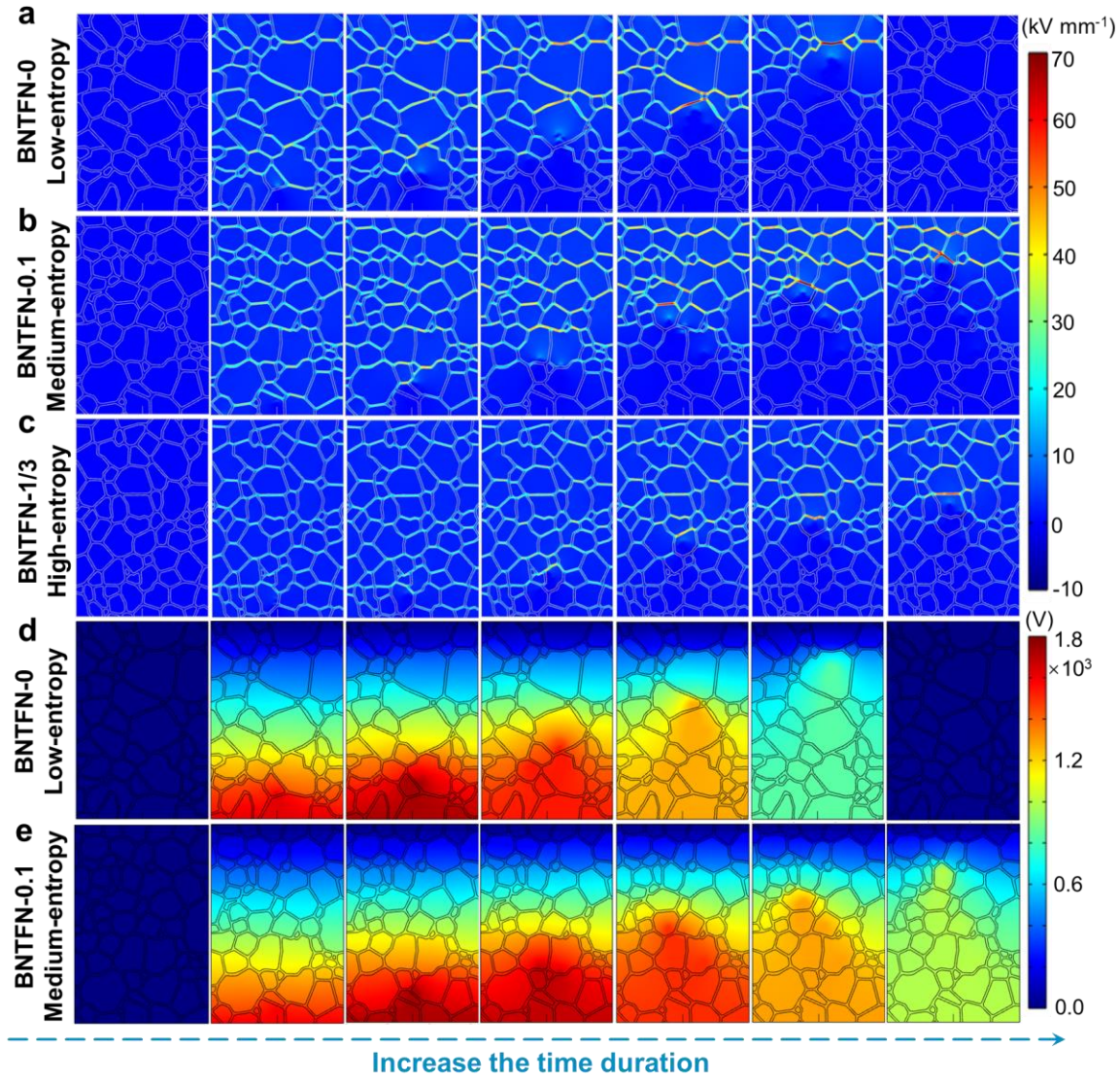

Fig. S8 Electric field distribution for **a** BNTFN-0, **b** BNTFN-0.1, and **c** BNTFN-1/3 ceramics from low-entropy to high-entropy. Electric potential distribution for **d** BNTFN-0 and **e** BNTFN-0.1 ceramic

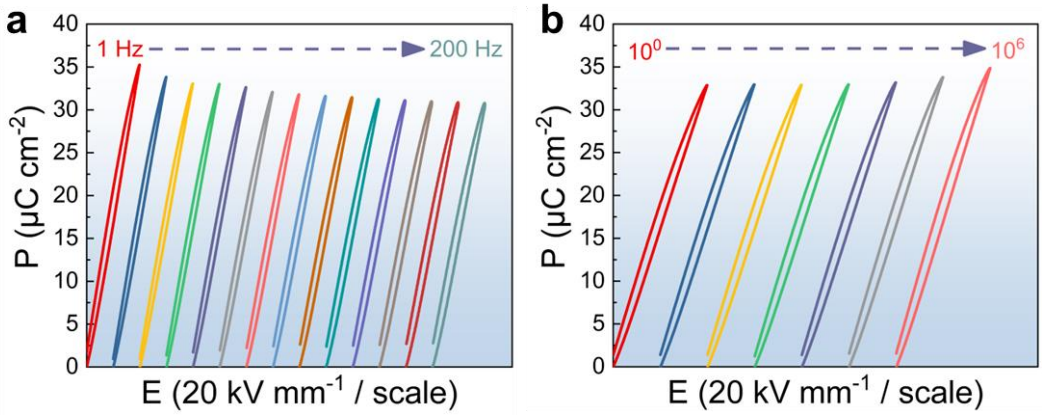

Fig. S9 a Frequency-dependent *P*-*E* loops under 40 kV mm^{-1} for BNTFN-1/3 ceramic. **b** *P*-*E* loops as a function of the cycle number under 40 kV mm^{-1} for BNTFN-1/3 ceramic

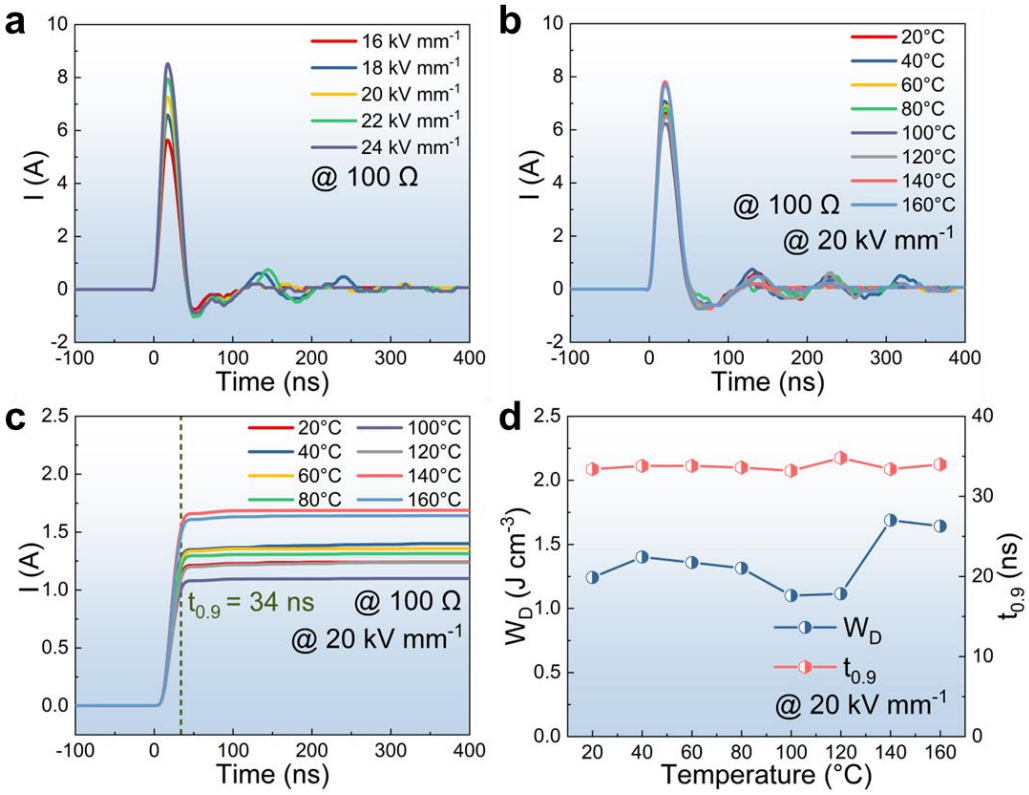

Fig. S10 **a** Overdamped discharge waveforms for BNTFN-1/3 ceramic. **b** Overdamped discharge waveforms, **c** Calculated overdamped discharge density W_D, and **d** W_D and $t_{0.9}$ values at 20 kV mm^{-1} under different temperature for the BNTFN-1/3 ceramic (R_o =100 Ω)

The discharge energy density W_D can be calculated using the following formulas:

$$W_D = \frac{R_o \int I_{(t)}^2 dt}{V} \qquad (6)$$

where V is the sample volume.

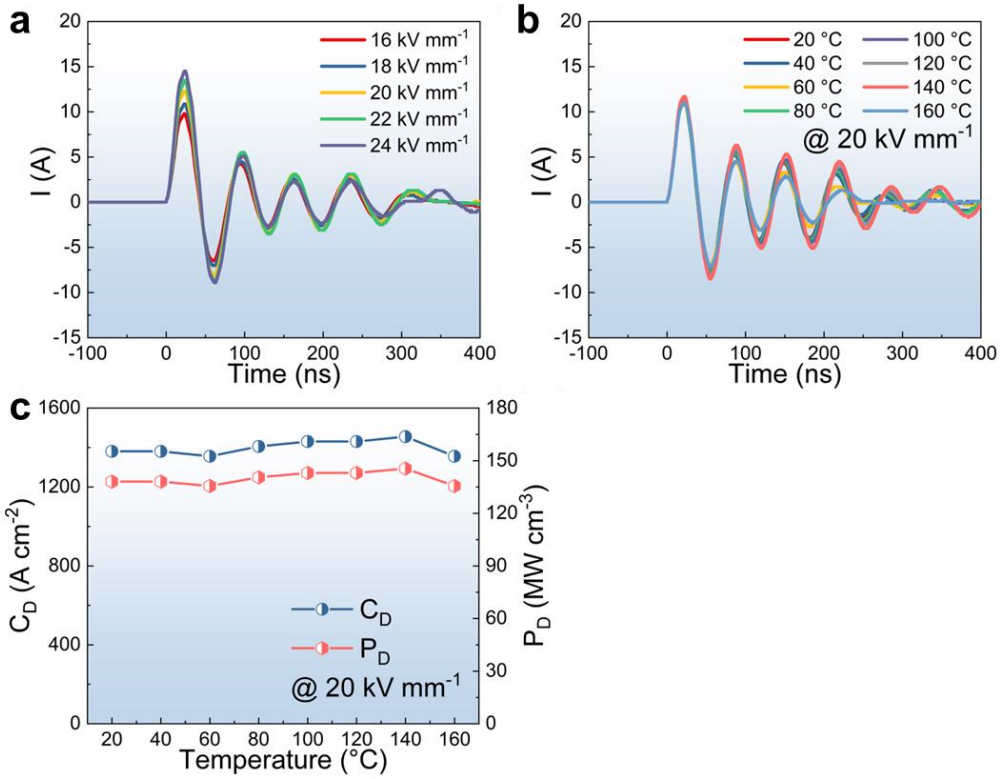

Fig. S11 **a** Underdamped discharge waveforms for BNTFN-1/3 ceramic. **b** Underdamped discharge waveforms, and **c** C_D and P_D values at 20 kV mm^{-1} under different temperatures

The current density C_D and power density P_D can be calculated using the following formulas:

$$C_D = \frac{I_{max}}{S} \quad (7)$$

$$P_D = \frac{E \times I_{max}}{2S} \quad (8)$$

where S is the electrode area.

Table S1 Relevant references for the Fig. 2e,f.

Figure	***Ref.***
Fig. 2e,f	[6-195]

References

1. Z. Cai, X. Wang, W. Hong, B. Luo, Q. Zhao et al., Grain-size–dependent dielectric properties in nanograin ferroelectrics. J. Am. Ceram. Soc. **101**(12), 5487-5496 (2018).

2. Z. Cai, X. Wang, B. Luo, W. Hong, L. Wu et al., Dielectric response and breakdown behavior of polymer-ceramic nanocomposites: The effect of nanoparticle distribution. Compos. Sci. Technol. **145**, 105-113 (2017).

3. K.M. Johnson, Variation of dielectric constant with voltage in ferroelectrics and its application to parametric devices. J. Appl. Phys. **33**(9), 2826-2831 (1962).

4. X. Dong, X. Li, X. Chen, Z. Tan, J. Wu et al., (1-*x*)[0.90NN-0.10Bi($Mg_{2/3}Nb_{1/3}$)O_3]-*x*($Bi_{0.5}Na_{0.5}$)$_{0.7}Sr_{0.3}TiO_3$ ceramics with core–shell structures: A pathway for simultaneously achieving high polarization and breakdown strength. Nano Energy **101**, 107577 (2022).

5. L. Padurariu, L. Curecheriu, V. Buscaglia, L. Mitoseriu, Field-dependent permittivity in nanostructured $BaTiO_3$ ceramics: Modeling and experimental verification. Phys. Rev. B **85**(22), 224111 (2012).

6. W. Liu, J. Gao, Y. Zhao, S. Li, Significant enhancement of energy storage properties of $BaTiO_3$-based ceramics by hybrid-doping. J. Alloys Compd. **843**, 155938 (2020).

7. D. Zhan, Q. Xu, D.-P. Huang, H.-X. Liu, W. Chen et al., Dielectric nonlinearity and electric breakdown behaviors of $Ba_{0.95}Ca_{0.05}Zr_{0.3}Ti_{0.7}O_3$ ceramics for energy storage utilizations. J. Alloys Compd. **682**, 594-600 (2016).

8. Z. Shen, X. Wang, B. Luo, L. Li, $BaTiO_3$–$BiYbO_3$ perovskite materials for energy storage applications. J. Mater. Chem. A **3**(35), 18146-18153 (2015).

9. X. Yi, C. Ji, G. Chen, H. Yang, H. Yong et al., Wang, Effects of Sintering Method and $BiAlO_3$ Dopant on Dielectric Relaxation and Energy Storage Properties of $BaTiO_3$–$BiYbO_3$ Ceramics.

physica status solidi (a) **217**(2), 1900721 (2020).

10. T. Wang, L. Jin, C. Li, Q. Hu, X. Wei, Relaxor ferroelectric $BaTiO_3$–$Bi(Mg_{2/3}Nb_{1/3})O_3$ ceramics for energy storage application. J. Am. Ceram. Soc. **98**(2), 559-566 (2015).

11. Z. Sun, L. Li, S. Yu, X. Kang, S. Chen, Energy storage properties and relaxor behavior of lead-free $Ba_{1-x}Sm_{2x/3}Zr_{0.15}Ti_{0.85}O_3$ ceramics. Dalt. Trans. **46**(41), 14341-14347 (2017).

12. X. Jiang, H. Hao, S. Zhang, J. Lv, M. Cao et al., Enhanced energy storage and fast discharge properties of $BaTiO_3$ based ceramics modified by $Bi(Mg_{1/2}Zr_{1/2})O_3$. J. Eur. Ceram. Soc. **39**(4), 1103-1109 (2019).

13. X. Liu, H. Yang, F. Yan, Y. Qin, Y. Lin et al., Enhanced energy storage properties of $BaTiO_3$-$Bi_{0.5}Na_{0.5}TiO_3$ lead-free ceramics modified by $SrY_{0.5}Nb_{0.5}O_3$. J. Alloys Compd. **778**, 97-104 (2019).

14. C. Zhu, Z. Cai, L. Li, X. Wang, High energy density, high efficiency and excellent temperature stability of lead free Mn–doped $BaTiO_3$–$Bi(Mg_{1/2}Zr_{1/2})O_3$ ceramics sintered in a reducing atmosphere. J. Alloys Compd. **816**, 152498 (2020).

15. L. Zhang, L.-X. Pang, W.-B. Li, D. Zhou, Extreme high energy storage efficiency in perovskite structured $(1-x)(Ba_{0.8}Sr_{0.2})TiO_3$-$xBi(Zn_{2/3}Nb_{1/3})O_3$ ($0.04\leq x\leq 0.16$) ceramics. J. Eur. Ceram. Soc. **40**(8), 3343-3347 (2020).

16. W.-B. Li, D. Zhou, L.-X. Pang, Enhanced energy storage density by inducing defect dipoles in lead free relaxor ferroelectric $BaTiO_3$-based ceramics. Appl. Phys. Lett. **110**(13), 132902 (2017).

17. Y. Li, J. Bian, Effects of reoxidation on the dielectric and energy storage properties of Ce-doped (Ba,Sr)TiO_3 ceramics prepared by hot-pressed sintering. J. Eur. Ceram. Soc. **40**(15), 5441-5449 (2020).

18. Q. Hu, L. Jin, T. Wang, C. Li, Z. Xing et al., Dielectric and temperature stable energy storage properties of 0.88$BaTiO_3$–0.12Bi $(Mg_{1/2}Ti_{1/2})O_3$ bulk ceramics. J. Alloys Compd. **640**, 416-420 (2015).

19. A. Jain, Y. Wang, N. Wang, F. Wang, Critical role of CuO doping on energy storage performance and electromechanical properties of $Ba_{0.8}Sr_{0.1}Ca_{0.1}Ti_{0.9}Zr_{0.1}O_3$ ceramics. Ceram. Int. **46**(11), 18800-18812 (2020).

20. G. Liu, Y. Li, M. Shi, L. Yu, P. Chen et al., An investigation of the dielectric energy storage performance of $Bi(Mg_{2/3}Nb_{1/3})O_3$-modifed $BaTiO_3$ Pb-free bulk ceramics with improved temperature/frequency stability. Ceram. Int. **45**(15), 19189-19196 (2019).

21. H. Yang, F. Yan, Y. Lin, T. Wang, Enhanced energy storage properties of $Ba_{0.4}Sr_{0.6}TiO_3$ lead-free ceramics with Bi_2O_3-B_2O_3-SiO_2 glass addition. J. Eur. Ceram. Soc. **38**(4), 1367-1373 (2018).

22. W.-B. Li, D. Zhou, L.-X. Pang, Structure and energy storage properties of Mn-doped (Ba,Sr)TiO_3–MgO composite ceramics. J. Mater. Sci.: Mater. Electron. **28**(12), 8749-8754 (2017).

23. Z. Dai, J. Xie, X. Fan, X. Ding, W. Liu et al., Enhanced energy storage properties and stability of $Sr(Sc_{0.5}Nb_{0.5})O_3$ modified 0.65$BaTiO_3$-0.35$Bi_{0.5}Na_{0.5}TiO_3$ ceramics. Chem. Eng. J. **397**, 125520 (2020).

24. Y. Huang, C. Zhao, B. Wu, J. Wu, Multifunctional $BaTiO_3$-based relaxor ferroelectrics toward excellent energy storage performance and electrostrictive strain benefiting from crossover region. ACS Appl. Mater. Interfaces **12**(21), 23885-23895 (2020).

25. M. Zhou, R. Liang, Z. Zhou, X. Dong, Combining high energy efficiency and fast charge-discharge capability in novel $BaTiO_3$-based relaxor ferroelectric ceramic for energy-storage. Ceram. Int. **45**(3), 3582-3590 (2019).

26. M. Zhou, R. Liang, Z. Zhou, X. Dong, Novel $BaTiO_3$-based lead-free ceramic capacitors featuring high energy storage density, high power density, and excellent stability. J. Mater. Chem. C **6**(31), 8528-8537 (2018).

27. F. Si, B. Tang, Z. Fang, H. Li, S. Zhang, A new type of $BaTiO_3$-based ceramics with $Bi(Mg_{1/2}Sn_{1/2})O_3$ modification showing improved energy storage properties and pulsed discharging performances. J. Alloys Compd. **819**, 153004 (2020).

28. Q. Wang, P.-M. Gong, C.-M. Wang, High recoverable energy storage density and large energy efficiency simultaneously achieved in $BaTiO_3$–$Bi(Zn_{1/2}Zr_{1/2})O_3$ relaxor ferroelectrics. Ceram. Int. **46**(14), 22452-22459 (2020).

29. X. Chen, X. Li, J. Sun, C. Sun, J. Shi et al., Achieving ultrahigh energy storage density and energy efficiency simultaneously in barium titanate based ceramics. Appl. Phys. A **126**(2), 1-8 (2020).

30. A. Jain, Y. Wang, H. Guo, Microstructural properties and ultrahigh energy storage density in $Ba_{0.9}Ca_{0.1}TiO_3$–$NaNb_{0.85}Ta_{0.15}O_3$ relaxor ceramics. Ceram. Int. **46**(15), 24333-24346 (2020).

31. F. Si, B. Tang, Z. Fang, H. Li, S. Zhang, Enhanced energy storage and fast charge-discharge properties of $(1-x)BaTiO_3$-$xBi(Ni_{1/2}Sn_{1/2})O_3$ relaxor ferroelectric ceramics. Ceram. Int. **45**(14), 17580-17590 (2019).

32. Q. Yuan, G. Li, F.-Z. Yao, S.-D. Cheng, Y. Wang et al., Simultaneously achieved temperature-insensitive high energy density and efficiency in domain engineered $BaTiO_3$-$Bi(Mg_{0.5}Zr_{0.5})O_3$ lead-free relaxor ferroelectrics. Nano Energy **52**, 203-210 (2018).

33. X. Li, X. Chen, J. Sun, M. Zhou, H. Zhou, Novel lead-free ceramic capacitors with high energy density and fast discharge performance. Ceram. Int. **46**(3), 3426-3432 (2020).

34. Y. Wang, S. Gao, T. Wang, J. Liu, D. Li et al., Structure, dielectric properties of novel $Ba(Zr,Ti)O_3$ based ceramics for energy storage application. Ceram. Int. **46**(8), 12080-12087

(2020).

35. X. Chen, X. Li, J. Sun, C. Sun, J. Shi et al., Simultaneously achieving ultrahigh energy storage density and energy efficiency in barium titanate based ceramics. Ceram. Int. **46**(3), 2764-2771 (2020).

36. Z. Dai, J. Xie, W. Liu, X. Wang, L. Zhang et al., Effective strategy to achieve excellent energy storage properties in lead-free $BaTiO_3$-based bulk ceramics. ACS Appl. Mater. Interfaces **12**(27), 30289-30296 (2020).

37. Z.-G. Liu, M.-D. Li, Z.-H. Tang, X.-G. Tang, Enhanced energy storage density and efficiency in lead-free $Bi(Mg_{1/2}Hf_{1/2})O_3$-modified $BaTiO_3$ ceramics. Chem. Eng. J. **418**, 129379 (2021).

38. G. Liu, Y. Li, B. Guo, M. Tang, Q. Li et al., Ultrahigh dielectric breakdown strength and excellent energy storage performance in lead-free barium titanate-based relaxor ferroelectric ceramics via a combined strategy of composition modification, viscous polymer processing, and liquid-phase sintering. Chem. Eng. J. **398**, 125625 (2020).

39. Z.-G. Liu, Z.-H. Tang, S.-C. Hu, D.-J. Yao, F. Sun et al., Excellent energy storage density and efficiency in lead-free Sm-doped $BaTiO_3$–$Bi(Mg_{0.5}Ti_{0.5})O_3$ ceramics. J. Mater. Chem. C **8**(38), 13405-13414 (2020).

40. D. Hu, Z. Pan, X. Tan, F. Yang, J. Ding et al., Optimization the energy density and efficiency of $BaTiO_3$-based ceramics for capacitor applications. Chem. Eng. J. **409**, 127375 (2021).

41. Y. Li, Y. Liu, M. Tang, J. Lv, F. Chen et al., Energy storage performance of $BaTiO_3$-based relaxor ferroelectric ceramics prepared through a two-step process. Chem. Eng. J. **419**, 129673 (2021).

42. X. Dong, X. Li, X. Chen, J. Wu, H. Zhou, Simultaneous enhancement of polarization and breakdown strength in lead-free $BaTiO_3$-based ceramics. Chem. Eng. J. **409**, 128231 (2021).

43. Q. Hu, Y. Tian, Q. Zhu, J. Bian, L. Jin et al., Achieve ultrahigh energy storage performance in $BaTiO_3$–$Bi(Mg_{1/2}Ti_{1/2})O_3$ relaxor ferroelectric ceramics via nano-scale polarization mismatch and reconstruction. Nano Energy **67**, 104264 (2020).

44. W. Huang, Y. Chen, X. Li, G. Wang, N. Liu et al., Ultrahigh recoverable energy storage density and efficiency in barium strontium titanate-based lead-free relaxor ferroelectric ceramics. Appl. Phys. Lett. **113**(20), 203902 (2018).

45. H. Yang, Z. Lu, L. Li, W. Bao, H. Ji et al., Novel $BaTiO_3$-based, Ag/Pd-compatible lead-free relaxors with superior energy storage performance. ACS Appl. Mater. Interfaces **12**(39), 43942-43949 (2020).

46. W. Wang, L. Zhang, R. Jing, Q. Hu, D. Alikin et al., Enhancement of energy storage performance in lead-free barium titanate-based relaxor ferroelectrics through a synergistic two-step strategy design. Chem. Eng. J. **434**, 134678 (2022).

47. W. Huang, Y. Chen, X. Li, G. Wang, J. Xia et al., Superior energy storage performances achieved in $(Ba,Sr)TiO_3$-based bulk ceramics through composition design and Core-shell structure engineering. Chem. Eng. J. **444**, 135523 (2022).

48. L. Li, X. Yu, H. Cai, Q. Liao, Y. Han et al., Preparation and dielectric properties of $BaCu(B_2O_5)$-doped $SrTiO_3$-based ceramics for energy storage. Mater. Sci. Eng.: B **178**(20), 1509-1514 (2013).

49. H. Yang, F. Yan, Y. Lin, T. Wang, L. He et al., A lead free relaxation and high energy storage efficiency ceramics for energy storage applications. J. Alloys Compd. **710**, 436-445 (2017).

50. J. Wang, H. Fan, B. Hu, H. Jiang, Enhanced energy-storage performance and temperature-stable dielectric properties of $(1-x)(0.94Na_{0.5}Bi_{0.5}TiO_3–0.06BaTiO_3)–xNa_{0.73}Bi_{0.09}NbO_3$ ceramics. J. Mater. Sci.: Mater. Electron. **30**(3), 2479-2488 (2019).

51. H. Wang, H. Yuan, X. Li, F. Zeng, K. Wu et al., Enhanced energy density and discharged

efficiency of lead-free relaxor (1-*x*)[($Bi_{0.5}Na_{0.5}$)$_{0.94}Ba_{0.06}$]$_{0.98}La_{0.02}TiO_3$-*x*$KNb_{0.6}Ta_{0.4}O_3$ ceramic capacitors. Chem. Eng. J. **394**, 124879 (2020).

52. P. Zhao, B. Tang, F. Si, C. Yang, H. Li et al., Novel Ca doped $Sr_{0.7}Bi_{0.2}TiO_3$ lead-free relaxor ferroelectrics with high energy density and efficiency. J. Eur. Ceram. Soc. **40**(5), 1938-1946 (2020).

53. Z. Chen, X. Bu, B. Ruan, J. Du, P. Zheng et al., Simultaneously achieving high energy storage density and efficiency under low electric field in $BiFeO_3$-based lead-free relaxor ferroelectric ceramics. J. Eur. Ceram. Soc. **40**(15), 5450-5457 (2020).

54. R. Kang, Z. Wang, W. Liu, L. He, X. Zhu et al., Domain engineered lead-free ceramics with large energy storage density and ultra-high efficiency under low electric fields. ACS Appl. Mater. Interfaces **13**(21), 25143-25152 (2021).

55. X. Kong, L. Yang, Z. Cheng, S. Zhang, Bi-modified $SrTiO_3$-based ceramics for high-temperature energy storage applications. J. Am. Ceram. Soc. **103**(3), 1722-1731 (2020).

56. Y. Huang, Q. Guo, H. Hao, H. Liu, S. Zhang, Tailoring properties of ($Bi_{0.51}Na_{0.47}$)TiO_3 based dielectrics for energy storage applications. J. Eur. Ceram. Soc. **39**(15), 4752-4760 (2019).

57. Y. Pu, W. Wang, X. Guo, R. Shi, M. Yang et al., Enhancing the energy storage properties of $Ca_{0.5}Sr_{0.5}TiO_3$-based lead-free linear dielectric ceramics with excellent stability through regulating grain boundary defects. J. Mater. Chem. C **7**(45), 14384-14393 (2019).

58. L. Yang, X. Kong, Z. Cheng, S. Zhang, Ultra-high energy storage performance with mitigated polarization saturation in lead-free relaxors. J. Mater. Chem. A **7**(14), 8573-8580 (2019).

59. M. Zhou, R. Liang, Z. Zhou, X. Dong, Achieving ultrahigh energy storage density and energy efficiency simultaneously in sodium niobate-based lead-free dielectric capacitors via microstructure modulation. Inorg. Chem. Fron. **6**(8), 2148-2157 (2019).

60. X. Zhang, D. Hu, Z. Pan, X. Lv, Z. He et al., Enhancement of recoverable energy density and efficiency of lead-free relaxor-ferroelectric BNT-based ceramics. Chem. Eng. J. **406**, 126818 (2021).

61. X. Qiao, F. Zhang, D. Wu, B. Chen, X. Zhao et al., Superior comprehensive energy storage properties in $Bi_{0.5}Na_{0.5}TiO_3$-based relaxor ferroelectric ceramics. Chem. Eng. J. **388**, 124158 (2020).

62. T. Wei, K. Liu, P. Fan, D. Lu, B. Ye et al., Novel $NaNbO_3$–$Sr_{0.7}Bi_{0.2}TiO_3$ lead-free dielectric ceramics with excellent energy storage properties. Ceram. Int. **47**(3), 3713-3719 (2021).

63. F. Yan, K. Huang, T. Jiang, X. Zhou, Y. Shi et al., Significantly enhanced energy storage density and efficiency of BNT-based perovskite ceramics via A-site defect engineering. Energy Storage Mater. **30**, 392-400 (2020).

64. H. Ji, D. Wang, W. Bao, Z. Lu, G. Wang et al., Ultrahigh energy density in short-range tilted NBT-based lead-free multilayer ceramic capacitors by nanodomain percolation. Energy Storage Mater. **38**, 113-120 (2021).

65. H. Chen, J. Shi, X. Chen, C. Sun, F. Pang et al., Excellent energy storage properties and stability of $NaNbO_3$–$Bi(Mg_{0.5}Ta_{0.5})O_3$ ceramics by introducing $(Bi_{0.5}Na_{0.5})_{0.7}Sr_{0.3}TiO_3$. J. Mater. Chem. A **9**(8), 4789-4799 (2021).

66. H. Qi, A. Xie, A. Tian, R. Zuo, Superior energy-storage capacitors with simultaneously giant energy density and efficiency using nanodomain engineered $BiFeO_3$-$BaTiO_3$-$NaNbO_3$ lead-free bulk ferroelectrics. Adv. Energy Mater. **10**(6), 1903338 (2020).

67. N. Luo, K. Han, F. Zhuo, C. Xu, G. Zhang et al., Aliovalent A-site engineered $AgNbO_3$ lead-free antiferroelectric ceramics toward superior energy storage density. J. Mater. Chem. A **7**(23), 14118-14128 (2019).

68. J. Gao, L. Zhao, Q. Liu, X. Wang, S. Zhang et al., Antiferroelectric-ferroelectric phase

transition in lead-free $AgNbO_3$ ceramics for energy storage applications. J. Am. Ceram. Soc. **101**(12), 5443-5450 (2018).

69. N. Luo, K. Han, M.J. Cabral, X. Liao, S. Zhang et al., Constructing phase boundary in $AgNbO_3$ antiferroelectrics: pathway simultaneously achieving high energy density and efficiency. Nature Commun. **11**, 4824 (2020).

70. S. Mao, N. Luo, K. Han, Q. Feng, X. Chen et al., Effect of Lu doping on the structure, electrical properties and energy storage performance of $AgNbO_3$ antiferroelectric ceramics. J. Mater. Sci.: Mater. Electron. **31**(10), 7731-7741 (2020).

71. A. Song, J. Song, Y. Lv, L. Liang, J. Wang et al., Energy storage performance in $BiMnO_3$-modified $AgNbO_3$ anti-ferroelectric ceramics. Mater. Lett. **237**, 278-281 (2019).

72. J. Gao, Y. Zhang, L. Zhao, K.-Y. Lee, Q. Liu et al., Enhanced antiferroelectric phase stability in La-doped $AgNbO_3$: perspectives from the microstructure to energy storage properties. J. Mater. Chem. A **7**(5), 2225-2232 (2019).

73. P. Ren, D. Ren, L. Sun, F. Yan, S. Yang et al., Grain size tailoring and enhanced energy storage properties of two-step sintered Nd^{3+}-doped $AgNbO_3$. J. Eur. Ceram. Soc. **40**(13), 4495-4502 (2020).

74. Y. Tian, L. Jin, H. Zhang, Z. Xu, X. Wei et al., High energy density in silver niobate ceramics. J. Mater. Chem. A **4**(44), 17279-17287 (2016).

75. Y. Xu, Y. Guo, Q. Liu, G. Wang, J. Bai et al., High energy storage properties of lead-free Mn-doped (1-*x*)$AgNbO_3$-*x*$Bi_{0.5}Na_{0.5}TiO_3$ antiferroelectric ceramics. J. Eur. Ceram. Soc. **40**(1), 56-62 (2020).

76. C. Xu, Z. Fu, Z. Liu, L. Wang, S. Yan et al., La/Mn codoped $AgNbO_3$ lead-free antiferroelectric ceramics with large energy density and power density. ACS Sustainable Chem. Eng. **6**(12), 16151-16159 (2018).

77. N. Luo, K. Han, L. Liu, B. Peng, X. Wang et al., Lead-free $Ag_{1-3x}La_xNbO_3$ antiferroelectric ceramics with high-energy storage density and efficiency. J. Am. Ceram. Soc. **102**(8), 4640-4647 (2019).

78. L. Zhao, Q. Liu, S. Zhang, J.-F. Li, Lead-free $AgNbO_3$ anti-ferroelectric ceramics with an enhanced energy storage performance using MnO_2 modification. J. Mater. Chem. C **4**(36), 8380-8384 (2016).

79. L. Zhao, Q. Liu, J. Gao, S. Zhang, J.F. Li, Lead-free antiferroelectric silver niobate tantalate with high energy storage performance. Adv. Mater. **29**(31), 1701824 (2017).

80. J. Gao, Q. Liu, J. Dong, X. Wang, S. Zhang et al., Local structure heterogeneity in Sm-doped $AgNbO_3$ for improved energy-storage performance. ACS Appl. Mater. Interfaces **12**(5), 6097-6104 (2020).

81. Z. Lu, W. Bao, G. Wang, S.-K. Sun, L. Li et al., Mechanism of enhanced energy storage density in $AgNbO_3$-based lead-free antiferroelectrics. Nano Energy **79**, 105423 (2021).

82. Y. Tian, L. Jin, H. Zhang, Z. Xu, X. Wei et al., Phase transitions in bismuth-modified silver niobate ceramics for high power energy storage. J. Mater. Chem. A **5**(33), 17525-17531 (2017).

83. K. Han, N. Luo, S. Mao, F. Zhuo, X. Chen et al., Realizing high low-electric-field energy storage performance in $AgNbO_3$ ceramics by introducing relaxor behaviour. J. Materiomics **5**(4), 597-605 (2019).

84. S. Li, H. Nie, G. Wang, C. Xu, N. Liu et al., Significantly enhanced energy storage performance of rare-earth-modified silver niobate lead-free antiferroelectric ceramics via local chemical pressure tailoring. J. Mater. Chem. C **7**(6), 1551-1560 (2019).

85. Z. Yan, D. Zhang, X. Zhou, H. Qi, H. Luo et al., Silver niobate based lead-free ceramics with high energy storage density. J. Mater. Chem. A **7**(17), 10702-10711 (2019).

86. L. Zhao, J. Gao, Q. Liu, S. Zhang, J.-F. Li, Silver niobate lead-free antiferroelectric ceramics: enhancing energy storage density by B-site doping. ACS Appl. Mater. Interfaces **10**(1), 819-826 (2018).

87. K. Han, N. Luo, S. Mao, F. Zhuo, L. Liu et al., Ultrahigh energy-storage density in A-/B-site co-doped $AgNbO_3$ lead-free antiferroelectric ceramics: insight into the origin of antiferroelectricity, J. Mater. Chem. A **7**(46), 26293-26301 (2019).

88. S. Li, T. Hu, H. Nie, Z. Fu, C. Xu et al., Giant energy density and high efficiency achieved in silver niobate-based lead-free antiferroelectric ceramic capacitors via domain engineering. Energy Storage Mater. **34**, 417-426 (2021).

89. W. Chao, T. Yang, Y. Li, Z. Liu, Enhanced energy storage density in Ca and Ta co-doped $AgNbO_3$ antiferroelectric ceramics. J. Am. Ceram. Soc. **103**(12), 7283-7290 (2020).

90. W. Chao, J. Gao, T. Yang, Y. Li, Excellent energy storage performance in La and Ta co-doped $AgNbO_3$ antiferroelectric ceramics. J. Eur. Ceram. Soc. **41**(15), 7670-7677 (2021).

91. J. Li, Y. Tian, Y. Lan, L. Jin, C. Chen et al., Silver deficiency effect on dielectric properties and energy storage performance of $AgNbO_3$ ceramics. Ceram. Int. **47**(18), 26178-26184 (2021).

92. P. Shi, X. Wang, X. Lou, C. Zhou, Q. Liu et al., Significantly enhanced energy storage properties of Nd^{3+} doped $AgNbO_3$ lead-free antiferroelectric ceramics. J. Alloys Compd. **877**, 160162 (2021).

93. N. Luo, X. Tang, K. Han, L. Ma, Z. Chen et al., Silver stoichiometry engineering: an alternative way to improve energy storage density of $AgNbO_3$-based antiferroelectric ceramics. J. Mater. Res. **36**(5), 1067-1075 (2021).

94. Y. Xu, Y. Guo, Q. Liu, Y. Yin, J. Bai et al., Enhanced energy density in Mn-doped (1-*x*)$AgNbO_3$-*x*$CaTiO_3$ lead-free antiferroelectric ceramics. J. Alloys Compd. **821**, 153260 (2020).

95. N. Liu, R. Liang, Z. Zhou, X. Dong, Designing lead-free bismuth ferrite-based ceramics learning from relaxor ferroelectric behavior for simultaneous high energy density and efficiency under low electric field. J. Mater. Chem. C **6**(38), 10211-10217 (2018).

96. D. Zheng, R. Zuo, Enhanced energy storage properties in $La(Mg_{1/2}Ti_{1/2})O_3$-modified $BiFeO_3$-$BaTiO_3$ lead-free relaxor ferroelectric ceramics within a wide temperature range. J. Eur. Ceram. Soc. **37**(1), 413-418 (2017).

97. S. Dabas, M. Kumar, P. Chaudhary, O. Thakur, Enhanced magneto-electric coupling and energy storage analysis in Mn-modified lead free $BiFeO_3$-$BaTiO_3$ solid solutions. J. Appl. Phys. **126**(13), 134102 (2019).

98. D. Wang, Z. Fan, W. Li, D. Zhou, A. Feteira et al., High energy storage density and large strain in Bi $(Zn_{2/3}Nb_{1/3})O_3$-doped $BiFeO_3$–$BaTiO_3$ ceramics. ACS Appl. Energy Mater. **1**(8), 4403-4412 (2018).

99. F. Akram, J. Kim, S.A. Khan, A. Zeb, H.G. Yeo et al., Less temperature-dependent high dielectric and energy-storage properties of eco-friendly $BiFeO_3$–$BaTiO_3$-based ceramics. J. Alloys Compd. **818**, 152878 (2020).

100. D. Zheng, R. Zuo, D. Zhang, Y. Li, Novel $BiFeO_3$–$BaTiO_3$–$Ba(Mg_{1/3}Nb_{2/3})O_3$ lead-free relaxor ferroelectric ceramics for energy-storage capacitors. J. Am. Ceram. Soc. **98**(9), 2692-2695 (2015).

101. N. Liu, R. Liang, X. Zhao, C. Xu, Z. Zhou et al., Novel bismuth ferrite-based lead-free ceramics with high energy and power density. J. Am. Ceram. Soc. **101**(8), 3259-3265 (2018).

102. Z. Lu, G. Wang, W. Bao, J. Li, L. Li et al., Superior energy density through tailored dopant strategies in multilayer ceramic capacitors. Energy Environ. Sci. **13**(9), 2938-2948 (2020).

103. Z. Chen, X. Bai, H. Wang, J. Du, W. Bai et al., Achieving high-energy storage performance in $0.67Bi_{1-x}Sm_xFeO_3$-$0.33BaTiO_3$ lead-free relaxor ferroelectric ceramics. Ceram. Int. **46**(8),

11549-11555 (2020).

104. H. Yang, H. Qi, R. Zuo, Enhanced breakdown strength and energy storage density in a new $BiFeO_3$-based ternary lead-free relaxor ferroelectric ceramic. J. Eur. Ceram. Soc. **39**(8), 2673-2679 (2019).

105. G. Wang, Z. Lu, H. Yang, H. Ji, A. Mostaed et al., Fatigue resistant lead-free multilayer ceramic capacitors with ultrahigh energy density. J. Mater. Chem. A **8**(22), 11414-11423 (2020).

106. H. Sun, X. Wang, Q. Sun, X. Zhang, Z. Ma et al., Large energy storage density in $BiFeO_3$-$BaTiO_3$-$AgNbO_3$ lead-free relaxor ceramics. J. Eur. Ceram. Soc. **40**(8), 2929-2935 (2020).

107. X. Bai, Z. Chen, P. Zheng, W. Bai, J. Zhang et al., High recoverable energy storage density in nominal (0.67-*x*)$BiFeO_3$-0.33$BaTiO_3$-*x*$BaBi_2Nb_2O_9$ lead-free composite ceramics. Ceram. Int. **47**(16), 23116-23123 (2021).

108. M. Shiga, M. Hagiwara, S. Fujihara, $(Bi_{1/2}K_{1/2})TiO_3$–$SrTiO_3$ solid-solution ceramics for high-temperature capacitor applications. Ceram. Int. **46**(8), 10242-10249 (2020).

109. F. Li, T. Jiang, J. Zhai, B. Shen, H. Zeng, Exploring novel bismuth-based materials for energy storage applications. J. Mater. Chem. C **6**(30), 7976-7981 (2018).

110. F. Li, X. Hou, T. Li, R. Si, C. Wang et al., Fine-grain induced outstanding energy storage performance in novel $Bi_{0.5}K_{0.5}TiO_3$–$Ba(Mg_{1/3}Nb_{2/3})O_3$ ceramics via a hot-pressing strategy. J. Mater. Chem. C **7**(39), 12127-12138 (2019).

111. F. Li, R. Si, T. Li, C. Wang, J. Zhai, High energy storage performance and fast discharging speed in dense 0.7$Bi_{0.5}K_{0.5}TiO_3$-0.3$SrTiO_3$ ceramics via a novel rolling technology. Ceram. Int. **46**(5), 6995-6998 (2020).

112. P. Zhao, B. Tang, Z. Fang, F. Si, C. Yang et al., Improved dielectric breakdown strength and energy storage properties in Er2O3 modified $Sr_{0.35}Bi_{0.35}K_{0.25}TiO_3$. Chem. Eng. J. **403**,

126290 (2021).

113. Q. Yang, M. Zhu, Q. Wei, M. Zhang, M. Zheng et al., Excellent energy storage performance of $K_{0.5}Bi_{0.5}TiO_3$-based ferroelectric ceramics under low electric field. Chem. Eng. J. **414**, 128769 (2021).

114. L. Chen, F. Long, H. Qi, H. Liu, S. Deng et al., Outstanding Energy Storage Performance in High-Hardness $(Bi_{0.5}K_{0.5})TiO_3$-Based Lead-Free Relaxors via Multi-Scale Synergistic Design. Adv. Funct. Mater. **32**(9), 2110478 (2022).

115. D. Hu, Z. Pan, X. Zhang, H. Ye, Z. He et al., Greatly enhanced discharge energy density and efficiency of novel relaxation ferroelectric BNT–BKT-based ceramics. J. Mater. Chem. C **8**(2), 591-601 (2020).

116. T. Li, P. Chen, R. Si, F. Li, Y. Guo et al., High energy storage density and efficiency with excellent temperature and frequency stabilities under low operating field achieved in $Ag_{0.91}Sm_{0.03}NbO_3$-modified $Na_{0.5}Bi_{0.5}TiO_3$-$BaTiO_3$ ceramics. J. Mater. Sci.: Mater. Electron. **31**(19), 16928-16937 (2020).

117. F. Zhang, X. Qiao, Q. Shi, X. Chao, Z. Yang et al., High energy storage density realized in $Bi_{0.5}Na_{0.5}TiO_3$-based relaxor ferroelectric ceramics at ultralow sintering temperature. J. Eur. Ceram. Soc. **41**(1), 368-375 (2021).

118. B. Hu, H. Fan, L. Ning, Y. Wen, C. Wang, High energy storage performance of $[(Bi_{0.5}Na_{0.5})_{0.94}Ba_{0.06}]_{0.97}La_{0.03}Ti_{1-x}(Al_{0.5}Nb_{0.5})_xO_3$ ceramics with enhanced dielectric breakdown strength. Ceram. Int. **44**(13), 15160-15166 (2018).

119. C. Zhu, Z. Cai, B. Luo, L. Guo, L. Li et al., High temperature lead-free BNT-based ceramics with stable energy storage and dielectric properties. J. Mater. Chem. A **8**(2), 683-692 (2020).

120. L. Zhang, X. Pu, M. Chen, S. Bai, Y. Pu, Influence of $BaSnO_3$ additive on the energy

storage properties of $Na_{0.5}Bi_{0.5}TiO_3$-based relaxor ferroelectrics. J. Eur. Ceram. Soc. **38**(5), 2304-2311 (2018).

121. L. Zhang, Y. Pu, M. Chen, Influence of $BaZrO_3$ additive on the energy-storage properties of $0.775Na_{0.5}Bi_{0.5}TiO_3$-$0.225BaSnO_3$ relaxor ferroelectrics. J. Alloys Compd. **775**, 342-347 (2019).

122. Z. Liu, A. Zhang, S. Xu, J. Lu, B. Xie et al., Mediating the confliction of polarizability and breakdown electric-field strength in BNST relaxor ferroelectric for energy storage applications. J. Alloys Compd. **823**, 153772 (2020).

123. J. Wu, A. Mahajan, L. Riekehr, H. Zhang, B. Yang et al., Perovskite $Sr_x(Bi_{1-x}Na_{0.97-x}Li_{0.03})_{0.5}TiO_3$ ceramics with polar nano regions for high power energy storage. Nano Energy **50**, 723-732 (2018).

124. D. Hu, Z. Pan, Z. He, F. Yang, X. Zhang et al., Significantly improved recoverable energy density and ultrafast discharge rate of $Na_{0.5}Bi_{0.5}TiO_3$-based ceramics. Ceram. Int. **46**(10), 15364-15371 (2020).

125. L. Zhang, Y. Pu, M. Chen, Ultra-high energy storage performance under low electric fields in $Na_{0.5}Bi_{0.5}TiO_3$-based relaxor ferroelectrics for pulse capacitor applications. Ceram. Int. **46**(1), 98-105 (2020).

126. J. Yin, Y. Zhang, X. Lv, J. Wu, Ultrahigh energy-storage potential under low electric field in bismuth sodium titanate-based perovskite ferroelectrics. J. Mater. Chem. A **6**(21), 9823-9832 (2018).

127. H. Qi, R. Zuo, Linear-like lead-free relaxor antiferroelectric $(Bi_{0.5}Na_{0.5})TiO_3$–$NaNbO_3$ with giant energy-storage density/efficiency and super stability against temperature and frequency. J. Mater. Chem. A **7**(8), 3971-3978 (2019).

128. C. Zhang, W. Xiao, F. Zeng, D. Su, K. Du et al., Superior energy-storage performance in

$0.85Bi_{0.5}Na_{0.5}TiO_3$–$0.15NaNbO_3$ lead-free ferroelectric ceramics via composition and microstructure engineering. J. Mater. Chem. A **9**(16), 10088-10094 (2021).

129. X. Zhou, H. Qi, Z. Yan, G. Xue, H. Luo et al., Superior thermal stability of high energy density and power density in domain-engineered $Bi_{0.5}Na_{0.5}TiO_3$–$NaTaO_3$ relaxor ferroelectrics. ACS Appl. Mater. Interfaces **11**(46), 43107-43115 (2019).

130. R. Kang, Z. Wang, X. Lou, W. Liu, P. Shi et al., Energy storage performance of $Bi_{0.5}Na_{0.5}TiO_3$-based relaxor ferroelectric ceramics with superior temperature stability under low electric fields. Chem. Eng. J. **410**, 128376 (2021).

131. Z. Jiang, Z. Yang, Y. Yuan, B. Tang, S. Zhang, High energy storage properties and dielectric temperature stability of (1-*x*)(0.8$Bi_{0.5}Na_{0.5}TiO_3$-0.2$Ba_{0.3}Sr_{0.7}TiO_3$)-*x*$NaNbO_3$ lead-free ceramics. J. Alloys Compd. **851**, 156821 (2021).

132. Z. He, S. Shi, Z. Pan, L. Tang, J. Zhao et al., Low electric field induced high energy storage capability of the free-lead relaxor ferroelectric 0.94$Bi_{0.5}Na_{0.5}TiO_3$-0.06$BaTiO_3$-based ceramics. Ceram. Int. **47**(8), 11611-11617 (2021).

133. M.K. Bilal, R. Bashir, S.U. Asif, J. Wang, W. Hu, Enhanced energy storage properties of 0.7$Bi_{0.5}Na_{0.5}TiO_3$-0.3$SrTiO_3$ ceramic through the addition of $NaNbO_3$. Ceram. Int. **47**(21), 30922-30928 (2021).

134. H. Yang, J. Tian, Y. Lin, J. Ma, Realizing ultra-high energy storage density of lead-free 0.76$Bi_{0.5}Na_{0.5}TiO_3$-0.24$SrTiO_3$-$Bi(Ni_{2/3}Nb_{1/3})O_3$ ceramics under low electric fields. Chem. Eng. J. **418**, 129337 (2021).

135. P. Shi, X. Zhu, X. Lou, B. Yang, X. Guo et al., $Bi_{0.5}Na_{0.5}TiO_3$-based lead-free ceramics with superior energy storage properties at high temperatures. Comp. Part B: Eng. **215**, 108815 (2021).

136. X. Guo, P. Shi, X. Lou, Q. Liu, H. Zuo, Superior energy storage properties in

(1−*x*)(0.65$Bi_{0.5}Na_{0.5}TiO_3$-0.35$Bi_{0.2}Sr_{0.7}TiO_3$)-*x*$CaZrO_3$ ceramics with excellent temperature stability. J. Alloys Compd. **876**, 160101 (2021).

137. M. Wang, Q. Feng, Y. Wei, N. Luo, C. Yuan et al., Relaxor ferroelectric $Bi_{0.5}Na_{0.5}TiO_3$–$Sr_{0.7}Nd_{0.2}TiO_3$ ceramics with high energy storage density and excellent stability under a low electric field. J. Phys. Chem. Solids **157**, 110209 (2021).

138. K. Yao, C. Zhou, J. Wang, Y. Tan, Q. Li et al., $Bi_{0.5}Na_{0.5}TiO_3$–$Sr_{0.85}Bi_{0.1}TiO_3$ ceramics with high energy storage properties and extremely fast discharge speed via regulating relaxation temperature. Ceram. Int. **47**(8), 11294-11303 (2021).

139. C. Zhu, Z. Cai, B. Luo, X. Cheng, L. Guo et al., Multiphase engineered BNT-based ceramics with simultaneous high polarization and superior breakdown strength for energy storage applications. ACS Appl. Mater. Interfaces **13**(24), 28484-28492 (2021).

140. L. Zheng, P. Sun, P. Zheng, W. Bai, L. Li et al., Significantly tailored energy-storage performances in $Bi_{0.5}Na_{0.5}TiO_3$–$SrTiO_3$-based relaxor ferroelectric ceramics by introducing bismuth layer-structured relaxor $BaBi_2Nb_2O_9$ for capacitor application. J. Mater. Chem. C **9**(15), 5234-5243 (2021).

141. B. Guo, Y. Yan, M. Tang, Z. Wang, Y. Li et al., Energy storage performance of $Na_{0.5}Bi_{0.5}TiO_3$ based lead-free ferroelectric ceramics prepared via non-uniform phase structure modification and rolling process. Chem. Eng. J. **420**, 130475 (2021).

142. M. Zhang, H. Yang, D. Li, Y. Lin, Excellent energy density and power density achieved in $K_{0.5}Na_{0.5}NbO_3$-based ceramics with high optical transparency. J. Alloys Compd. **829**, 154565 (2020).

143. M. Zhang, H. Yang, D. Li, L. Ma, Y. Lin, Giant energy storage efficiency and high recoverable energy storage density achieved in $K_{0.5}Na_{0.5}NbO_3$-$Bi(Zn_{0.5}Zr_{0.5})O_3$ ceramics. J. Mater. Chem. C **8**(26), 8777-8785 (2020).

144. Z. Yang, F. Gao, H. Du, L. Jin, L. Yan et al., Grain size engineered lead-free ceramics with both large energy storage density and ultrahigh mechanical properties. Nano Energy **58**, 768-777 (2019).

145. Q. Chai, D. Yang, X. Zhao, X. Chao, Z. Yang, Lead-free (K,Na)NbO_3-based ceramics with high optical transparency and large energy storage ability. J. Am. Ceram. Soc. **101**(6), 2321-2329 (2018).

146. B. Qu, H. Du, Z. Yang, Lead-free relaxor ferroelectric ceramics with high optical transparency and energy storage ability. J. Mater. Chem. C **4**(9), 1795-1803 (2016).

147. Q. Jia, Y. Li, L. Guan, H. Sun, Q. Zhang et al., Photochromic and energy storage properties in $K_{0.5}Na_{0.5}NbO_3$-based ferroelectrics. J. Mater. Sci.: Mater. Electron. **31**(21), 19277-19292 (2020).

148. T. Shao, H. Du, H. Ma, S. Qu, J. Wang et al., Potassium–sodium niobate based lead-free ceramics: novel electrical energy storage materials. J. Mater. Chem. A **5**(2), 554-563 (2017).

149. Z. Yang, H. Du, S. Qu, Y. Hou, H. Ma et al., Significantly enhanced recoverable energy storage density in potassium–sodium niobate-based lead free ceramics. J. Mater. Chem. A **4**(36), 13778-13785 (2016).

150. B. Chen, Y. Tian, J. Lu, D. Wu, X. Qiao et al., Ultrahigh storage density achieved with (1-*x*)KNN-*x*BZN ceramics. J. Eur. Ceram. Soc. **40**(8), 2936-2944 (2020).

151. Y. Zhang, R. Zuo, Excellent energy-storage performances in La_2O_3 doped (Na,K)NbO_3-based lead-free relaxor ferroelectrics. J. Eur. Ceram. Soc. **40**(15), 5466-5474 (2020).

152. M. Zhang, H. Yang, Y. Yu, Y. Lin, Energy storage performance of $K_{0.5}Na_{0.5}NbO_3$-based ceramics modified by $Bi(Zn_{2/3}(Nb_{0.85}Ta_{0.15})_{1/3})O_3$. Chem. Eng. J. **425**, 131465 (2021).

153. J. Xing, Y. Huang, Q. Xu, B. Wu, Q. Zhang et al., Realizing high comprehensive energy

storage and ultrahigh hardness in lead-free ceramics. ACS Appl. Mater. Interfaces **13**(24), 28472-28483 (2021).

154. Z. Yang, H. Du, L. Jin, Q. Hu, S. Qu et al., A new family of sodium niobate-based dielectrics for electrical energy storage applications. J. Eur. Ceram. Soc. **39**(9), 2899-2907 (2019).

155. Y. Fan, Z. Zhou, R. Liang, X. Dong, Designing novel lead-free $NaNbO_3$-based ceramic with superior comprehensive energy storage and discharge properties for dielectric capacitor applications via relaxor strategy. J. Eur. Ceram. Soc. **39**(15), 4770-4777 (2019).

156. Z. Liu, J. Lu, Y. Mao, P. Ren, H. Fan, Energy storage properties of $NaNbO_3$-$CaZrO_3$ ceramics with coexistence of ferroelectric and antiferroelectric phases. J. Eur. Ceram. Soc. **38**(15), 4939-4945 (2018).

157. F. Pang, X. Chen, C. Sun, J. Shi, X. Li et al., Ultrahigh energy storage characteristics of sodium niobate-based ceramics by introducing a local random field. ACS Sustainable Chem. Eng. **8**(39), 14985-14995 (2020).

158. N. Qu, H. Du, X. Hao, A new strategy to realize high comprehensive energy storage properties in lead-free bulk ceramics. J. Mater. Chem. C **7**(26), 7993-8002 (2019).

159. J. Shi, X. Chen, X. Li, J. Sun, C. Sun et al., Realizing ultrahigh recoverable energy density and superior charge–discharge performance in $NaNbO_3$-based lead-free ceramics via a local random field strategy. J. Mater. Chem. C **8**(11), 3784-3794 (2020).

160. J. Shi, X. Chen, C. Sun, F. Pang, H. Chen et al., Superior thermal and frequency stability and decent fatigue endurance of high energy storage properties in $NaNbO_3$-based lead-free ceramics. Ceram. Int. **46**(16), 25731-25737 (2020).

161. R. Shi, Y. Pu, W. Wang, X. Guo, J. Li et al., A novel lead-free $NaNbO_3$–$Bi(Zn_{0.5}Ti_{0.5})O_3$ ceramics system for energy storage application with excellent stability. J. Alloys Compd. **815**,

152356 (2020).

162. L. Yang, X. Kong, Z. Cheng, S. Zhang, Enhanced energy storage performance of sodium niobate-based relaxor dielectrics by a ramp-to-spike sintering profile. ACS Appl. Mater. Interfaces **12**(29), 32834-32841 (2020).

163. Z. Yang, H. Du, L. Jin, Q. Hu, H. Wang et al., Realizing high comprehensive energy storage performance in lead-free bulk ceramics via designing an unmatched temperature range. J. Mater. Chem. A **7**(48), 27256-27266 (2019).

164. J. Ye, G. Wang, M. Zhou, N. Liu, X. Chen et al., Excellent comprehensive energy storage properties of novel lead-free $NaNbO_3$-based ceramics for dielectric capacitor applications. J. Mater. Chem. C **7**(19), 5639-5645 (2019).

165. M. Zhou, R. Liang, Z. Zhou, X. Dong, Superior energy storage properties and excellent stability of novel NaNbO 3-based lead-free ceramics with A-site vacancy obtained via a Bi_2O_3 substitution strategy. J. Mater. Chem. A **6**(37), 17896-17904 (2018).

166. M. Zhou, R. Liang, Z. Zhou, S. Yan, X. Dong, Novel sodium niobate-based lead-free ceramics as new environment-friendly energy storage materials with high energy density, high power density, and excellent stability. ACS Sustainable Chem. Eng. **6**(10), 12755-12765 (2018).

167. H. Qi, R. Zuo, A. Xie, A. Tian, J. Fu et al., Ultrahigh energy-storage density in $NaNbO_3$-based lead-free relaxor antiferroelectric ceramics with nanoscale domains. Adv. Funct. Mater. **29**(35), 1903877 (2019).

168. J. Chen, H. Qi, R. Zuo, Realizing Stable Relaxor Antiferroelectric and Superior Energy Storage Properties in $(Na_{1-x/2}La_{x/2})(Nb_{1-x}Ti_x)O_3$ Lead-Free Ceramics through A/B-Site Complex Substitution. ACS Appl. Mater. Interfaces **12**(29), 32871-32879 (2020).

169. A. Tian, R. Zuo, H. Qi, M. Shi, Large energy-storage density in transition-metal oxide modified $NaNbO_3$–$Bi(Mg_{0.5}Ti_{0.5})O_3$ lead-free ceramics through regulating the antiferroelectric

phase structure. J. Mater. Chem. A **8**(17), 8352-8359 (2020).

170. A. Xie, H. Qi, R. Zuo, Achieving Remarkable Amplification of energy-storage density in two-step sintered $NaNbO_3$–$SrTiO_3$ antiferroelectric capacitors through dual adjustment of local heterogeneity and grain scale. ACS Appl. Mater. Interfaces **12**(17), 19467-19475 (2020).

171. A. Xie, R. Zuo, Z. Qiao, Z. Fu, T. Hu et al., $NaNbO_3$-$(Bi_{0.5}Li_{0.5})TiO_3$ Lead-Free Relaxor Ferroelectric Capacitors with Superior Energy-Storage Performances via Multiple Synergistic Design. Adv. Energy Mater. **11**(28), 2101378 (2021).

172. H. Chen, X. Chen, J. Shi, C. Sun, X. Dong et al., Achieving ultrahigh energy storage density in $NaNbO_3$–$Bi(Ni_{0.5}Zr_{0.5})O_3$ solid solution by enhancing the breakdown electric field. Ceram. Int. **46**(18), 28407-28413 (2020).

173. X. Dong, X. Li, X. Chen, H. Chen, C. Sun et al., High energy storage density and power density achieved simultaneously in $NaNbO_3$-based lead-free ceramics via antiferroelectricity enhancement. J. Materiomics **7**(3), 629-639 (2021).

174. X. Dong, X. Li, X. Chen, H. Chen, C. Sun et al., High energy storage and ultrafast discharge in $NaNbO_3$-based lead-free dielectric capacitors via a relaxor strategy. Ceram. Int. **47**(3), 3079-3088 (2021).

175. J. Jiang, X. Meng, L. Li, J. Zhang, S. Guo et al., Enhanced energy storage properties of lead-free $NaNbO_3$-based ceramics via A/B-site substitution. Chem. Eng. J. **422**, 130130 (2021).

176. C. Sun, X. Chen, J. Shi, F. Pang, X. Dong et al., Simultaneously with large energy density and high efficiency achieved in $NaNbO_3$-based relaxor ferroelectric ceramics. J. Eur. Ceram. Soc. **41**(3), 1891-1903 (2021).

177. H. Chen, J. Shi, X. Dong, F. Pang, H. Zhang et al., Enhanced thermal and frequency stability and decent fatigue endurance in lead-free $NaNbO_3$-based ceramics with high energy storage density and efficiency. J. Materiomics **8**(2), 489-497 (2022).

178. F. Yan, H. Yang, Y. Lin, T. Wang, Dielectric and ferroelectric properties of $SrTiO_3$–$Bi_{0.5}Na_{0.5}TiO_3$–$BaAl_{0.5}Nb_{0.5}O_3$ lead-free ceramics for high-energy-storage applications. Inorg. Chem. **56**(21), 13510-13516 (2017).

179. W. Wang, Y. Pu, X. Guo, R. Shi, Y. Shi et al., Enhanced energy storage density and high efficiency of lead-free $Ca_{1-x}Sr_xTi_{1-y}Zr_yO_3$ linear dielectric ceramics. J. Eur. Ceram. Soc. **39**(16), 5236-5242 (2019).

180. L. Zhang, Z. Wang, Y. Li, P. Chen, J. Cai et al., Enhanced energy storage performance in Sn doped $Sr_{0.6}(Na_{0.5}Bi_{0.5})_{0.4}TiO_3$ lead-free relaxor ferroelectric ceramics. J. Eur. Ceram. Soc. **39**(10), 3057-3063 (2019).

181. W. Pan, M. Cao, A. Jan, H. Hao, Z. Yao et al., High breakdown strength and energy storage performance in (Nb,Zn) modified $SrTiO_3$ ceramics via synergy manipulation. J. Mater. Chem. C **8**(6), 2019-2027 (2020).

182. C. Cui, Y. Pu, R. Shi, High-energy storage performance in lead-free $(0.8-x)SrTiO_3$-$0.2Na_{0.5}Bi_{0.5}TiO_3$-$xBaTiO_3$ relaxor ferroelectric ceramics. J. Alloys Compd. **740**, 1180-1187 (2018).

183. H. Yang, F. Yan, Y. Lin, T. Wang, Improvement of dielectric and energy storage properties in $SrTiO_3$-based lead-free ceramics. J. Alloys Compd. **728**, 780-787 (2017).

184. C. Cui, Y. Pu, Z. Gao, J. Wan, Y. Guo et al., Structure, dielectric and relaxor properties in lead-free ST-NBT ceramics for high energy storage applications. J. Alloys Compd. **711**, 319-326 (2017).

185. X. Kong, L. Yang, Z. Cheng, S. Zhang, Ultrahigh energy storage properties in $(Sr_{0.7}Bi_{0.2})TiO_3$-$Bi(Mg_{0.5}Zr_{0.5})O_3$ lead-free ceramics and potential for high-temperature capacitors. Materials **13**(1), 180 (2020).

186. C. Cui, Y. Pu, Improvement of energy storage density with trace amounts of ZrO_2 additives

fabricated by wet-chemical method. J. Alloys Compd. **747**, 495-504 (2018).

187. H. Yang, F. Yan, Y. Lin, T. Wang, Enhanced recoverable energy storage density and high efficiency of $SrTiO_3$-based lead-free ceramics. Appl. Phys. Lett. **111**(25), 253903 (2017).

188. H. Yang, F. Yan, Y. Lin, T. Wang, Novel strontium titanate-based lead-free ceramics for high-energy storage applications. ACS Sustainable Chem. Eng. **5**(11), 10215-10222 (2017).

189. X. Guo, Y. Pu, W. Wang, J. Ji, J. Li et al., Ultrahigh energy storage performance and fast charge-discharge capability in Dy-modified $SrTiO_3$ linear ceramics with high optical transmissivity by defect and interface engineering. Ceram. Int. **46**(13), 21719-21727 (2020).

190. T. Cui, J. Zhang, J. Guo, X. Li, S. Guo et al., Outstanding comprehensive energy storage performance in lead-free $BiFeO_3$-based relaxor ferroelectric ceramics by multiple optimization design. Acta Mater. **240**, 118286 (2022).

191. T. Cui, J. Zhang, J. Guo, X. Li, S. Guo et al., Simultaneous achievement of ultrahigh energy storage density and high efficiency in $BiFeO_3$-based relaxor ferroelectric ceramics via a highly disordered multicomponent design. J. Mater. Chem. A **10**(27), 14316-14325 (2022).

192. K. Han, N. Luo, Y. Jing, X. Wang, B. Peng et al., Structure and energy storage performance of Ba-modified $AgNbO_3$ lead-free antiferroelectric ceramics. Ceram. Int. **45**(5), 5559-5565 (2019).

193. D. Wang, Z. Fan, D. Zhou, A. Khesro, S. Murakami et al., Bismuth ferrite-based lead-free ceramics and multilayers with high recoverable energy density. J. Mater. Chem. A **6**(9), 4133-4144 (2018).

194. A. Xie, J. Fu, R. Zuo, X. Jiang, T. Li et al., Supercritical relaxor nanograined ferroelectrics for ultrahigh-energy-storage capacitors. Adv. Mater. **34**, 2204356 (2022).

195. H. Tan, Z. Yan, S.-G. Chen, C. Samart, N. Takesue et al., SPS prepared NN-24SBT lead-

free relaxor-antiferroelectric ceramics with ultrahigh energy-storage density and efficiency. Scripta Mater. **210**, 114428 (2022).